DEVELOPMENT OF MODEL-BASED SENSORS AND THEIR USE FOR CLOSED-LOOP CONTROL OF SEPARATED SHEAR FLOWS

Ralf Becker, Maiko Garwon, and Rudibert King*

Measurement and Control Group, Institute for Process and Plant Technology, Sekr. P2-1,
Technical University Berlin
Hardenbergstraße 36a, D-10623 Berlin, Germany

* Corresponding author: fax ++49-30-314.21129; e-mail Rudibert.King@tu-berlin.de

Keywords: backward-facing step, reattachment length, robust, closed-loop control, Kalman filter

Abstract

Closed-loop control of separated flows is still hindered by a lack of fast and practical sensors for the measurement of the length of a separation bubble or of the position of reattachment. Therefore, a new real-time algorithm for the online detection of flow states is developed to overcome this limitation. For a model-based sensor microphone measurements in the separation zone are exploited and a control concept is outlined. The actuated backward-facing step flow is chosen as a benchmark configuration in which the length of the separated flow region is to be controlled. A closed-loop setup with a robust controller is implemented and studied experimentally showing a much better performance compared to a former approach. Based on the analysis of microphone signals a second model-based sensor for tracking of coherent vortical structures is proposed, too, and an extended control concept is outlined.

1 Introduction

Active flow control concepts have become an increasingly attractive topic in fluid mechanics in the last few years. When shaping of the geometry has reached an optimum or when passive means, such as vortex generators, have positive and negative effects, active devices in open- or closed-loop control can further improve the performance. The present investigation focusses on the closed-loop control of separated flows by such active means.

Feedback control of separated flows is not common in industrial applications yet, but has been proposed in the research community in the last few years. A literature survey on feedforward flow control including actuation mechanisms and sensor applications is given in Fiedler and Fernholz [4] and Gad-el-Hak et al. [5].

For feedback control three different approaches can be distinguished. On the one hand optimal control strategies on the basis of numerical solutions of the Navier-Stokes equations (NSE) are used. This is done by Hinze [9], for instance, who also gives a review about this field. These approaches are based on a detailed description of physical phenomena, but they are not applicable in real-time in the near future because of the enormous computational effort involved. On the other hand Allan et al. [1] and Becker et al. [2] propose low-dimensional black-box models for controller synthesis. Both groups implemented controllers in experiments in real-time. However, no physical sub-processes are resolved with the black-box models used thereby limiting the obtainable performance.

In a third approach low-dimensional models based on physical knowledge are derived with the intention to synthesise controllers. These Galerkin and vortex models for separation control are used by Gerhard et al. [7], and Pastoor et al. [14], respectively.

For studying the application of control methods for separated flows the backward-facing step is investigated here numerically and experimentally as a benchmark problem. The long-term objective is the establishment of a comparison of different control methods including new approaches for flow problems applicable in real-time, see as well the work in [2, 6, 7, 14].

The most common objective in the control of separated flows is the control of the size of the separation region. Thus the reattachment length x_R can be defined as a control variable. In Becker et al. [2] the time-mean reattachment length $\overline{x}_R$ is controlled by a feedback strategy with respect to a desired reference. Fig. 1 shows the tracking response. The control setup for the time-mean variable is very robust, but open- and closed-loop simulation studies based on the NSE revealed that a much faster behaviour of the instantaneous reattachment length x_R could be obtained. The reason for this slow experimental response is found in the time averaging of the measurement signal.

Based on these findings the paper is organized as follows: A concept for a faster extraction of information about x_R and a control of it are presented in section 3. In section 4 a second method for real-time tracking of the convecting periodic coherent vortical structures is proposed and its use for control is outlined. The flow configuration including a description of the sub-processes and the experimental setup are introduced in section 2, first. Finally, the results are summarized in section 5.

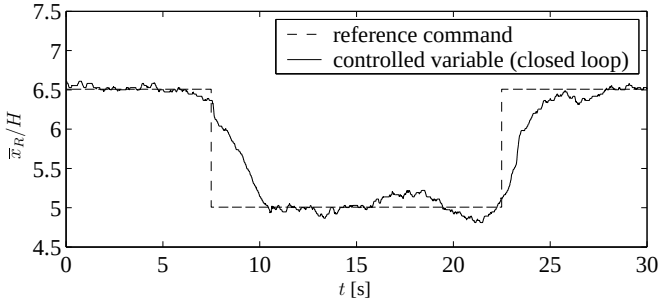

Figure 1: Tracking response of the controlled normalized time-mean reattachment length $\overline{x}_R$ of the prior investigations of Becker et al. [2] (experiment with $Re_H = 4000$)

2 Flow configuration

2.1 General description

The backward-facing step flow configuration has been established as a benchmark problem for separated flows in fluid mechanics first. A variety of information about the flow processes and actuation mechanisms is available, see for example Hasan [8] and Huppertz [10]. A sketch of the flow field is given in Fig. 2 where the rightwards moving flow with the free-stream velocity U_∞ detaches at the step edge. Three different regimes exist in the wake: a recirculation zone also called separation bubble with the shear layer above, a reattachment zone, and a boundary layer zone.

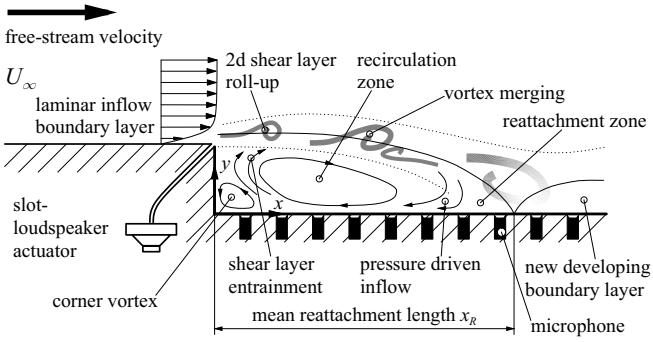

Figure 2: Flow field downstream of a backward-facing step

The shear layer is governed by the Kelvin-Helmholz instability phenomenon. Perturbations are amplified leading to vortex shedding with the natural frequency f_{shear}. Hence, the shear layer rolls up along the spanwise z-direction into two-dimensional, coherent vortical structures called vortices in the following. These vortices convect downstream with approximately the half free-stream velocity

$$c \approx U_\infty/2\,. \tag{1}$$

A recirculation bubble with pressure driven inflow, and outflow caused by shear layer entrainment exists in the wake. While negative skin-friction, i.e. reverse flow, occurs in the recirculation zone the reattachment position is characterized by zero friction. Downstream a new boundary layer develops causing positive skin-friction, i.e. forward flow.

Particularly the vortices are responsible for entrainment. By stimulating their growth or by merging two or more vortices into bigger structures the increased outflow leads to a significant reduction of the bubble size given by the length x_R.

The vortex generated entrainment mechanism is enhanced by the acoustic actuation of the detaching boundary layer at the step edge as shown in Fig. 2. A slot-loudspeaker actuator is used for this. As the Kelvin-Helmholz instability phenomenon is triggered by the input only a small amount of energy is needed which leads to an unstable growth of actuated perturbations. Therefore, the actuation frequency should be near the natural instability frequency, $f_{act} \approx f_{shear}$. The amplitude of the harmonic loudspeaker signal finally affects the initial size of the growing vortices and thus the reattachment length x_R.

Here x_R is defined as the first zero crossing from negative to positive skin-friction downstream of the global skin-friction minimum in the recirculation zone. Looking at simulated data both the temporal behaviour and the spatial structures are complicated due to the transitional behaviour of the flow behind the step. Every convecting vortex leads to one sawtooth-like temporal pattern by inducing backward flow at the wall, see also Kiya and Sasaki [11]. Neither the high-frequency sawtooth motion nor the mentioned irregular spatial distribution are controllable by the used acoustic actuation. After removing the temporal sawtooth motion from x_R a significant low-frequency flapping motion occurs which should be detected by the new sensor exploiting microphone signals and which should be controlled.

2.2 Setup and flow parameters

A Reynolds number of $Re_H = 4000$ corresponding to $U_\infty = 3.04$ m/s giving the dimensionless free-stream velocity ($Re_H = U_\infty H/\nu$) and a step height of $H = 20$ mm are chosen. All distances are made dimensionless by the step height H in the following.

Online sensor arrays with adequate time resolution which do not disturb the flow are needed for closed-loop control. Skin-friction sensors like hot wires, pulsed wires or classical surface fences, see Fernholz et al. [3], cannot be used for economical and practical reasons, especially with regard to the requirement of sensor arrays. A literature survey in Lee and Sung [12] reveals, however, that wall-pressure fluctuation measurements using microphone arrays in the wake are a utilizable concept. In the present investigation microphones are installed therefore in a streamwise centerline behind the step, see Fig. 2.

2.3 Characteristics of wall-pressure fluctuations

Based on the observation of Mabey [13] the streamwise root-mean-square (rms) distribution of the pressure fluctuations

p'_{rms} shows a significant maximum at 90% of the reattachment length $\overline{x}_R$ as shown in Fig. 3. Therefore, this measured distribution can be used to get information about x_R.

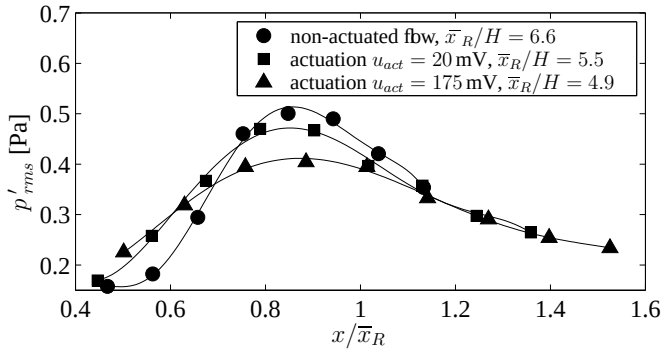

Figure 3: Streamwise distribution of rms pressure fluctuations (experiment with $Re_H = 4000$)

This sensor method is called the rms-method in the following and was successfully applied in Becker et al. [2] in closed-loop experiments. A moving window with a size of $3\,\text{s}$ was used for rms-calculation. Due to this averaging the temporal resolution of the rms-sensor limits the achievable performance as already mentioned, see Fig. 1. This can be concluded as well from step responses obtained numerically by solving the NSE which show that the time constants of the open-loop plant are in the order of $0.2\,\text{s}$.

However, pressure fluctuations p' measured by microphones contain instantaneous information of the velocity fluctuations of the whole flow field, too, including information coming from the spanwise vortices, see for example Lee and Sung [12].

As these vortices are responsible for the entrainment and hence for the reattachment length x_R the microphone measurements should be exploited in that respect in order to find correlations. Instantaneous features of flow variables are investigated in Lee and Sung [12] where two modes are found. Wall-pressure fluctuations p' in the recirculation and reattachment zone consist of a coherent mode from spanwise vortical structures called the vortex convection mode and a stationary mode which appears in all microphones nearly at the same time. Both modes are to be seen in the space-time contour plot of p' in Fig. 4. The vertical shaded patterns are the stationary mode whereas the vortex convection mode is given by the inclined contour pattern with the convection velocity $U_\infty/2$, see Eq. 1.

Convecting low pressure regions in Fig. 4 correspond to the centres of the spanwise vortical structures, see also Lee and Sung [12]. These minima are called vortex footprints and will be exploited in the sequel to get faster information about the reattachment length x_R.

For the quantitative analysis of vortex footprints the stationary mode is removed with a real-time algorithm. This idea was motivated by the work of Sonnenberger [15].

The vortex convection mode contains two utilizable features.

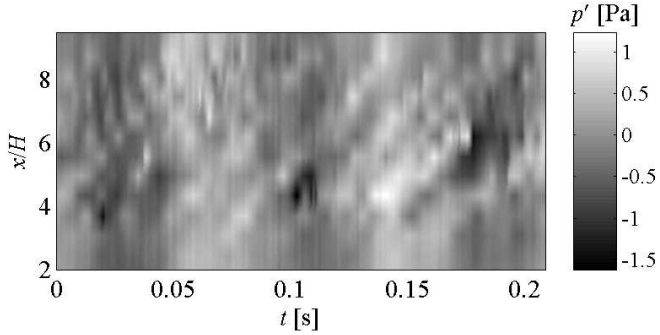

Figure 4: Space-time contour plot of wall-pressure fluctuationsp' (experiment with $Re_H = 4000$)

First, the courses of the vortices are given by the courses of the vortex footprints. A sensor algorithm for online and real-time tracking of multiple vortex objects can be proposed by running Kalman filters for each detected object. This approach is presented in section 4.

Second, the information of the footprint size can be exploited, too, to analyze the state of the spanwise vortices with a fast temporal resolution. This information on vortex development can be related to the bubble size and thus used in a controller as done in the section 3.

3 Vortex growing sensor and its use for reattachment length control

3.1 Kalman filter-based estimation of x_R

The position of a vortex structure, as outlined in section 2.3, can be obtained from the footprint signals, i.e. the time-dependent pressure signals, measured by the microphones. The depth of the footprints p_{env} is a measure of the size of the corresponding vortex structure. The depth can be determined by the difference between the actually detected minimum corresponding to the vortex convection mode and the last maximum of the pressure signal.

As the size of the separation zone is not determined by a single vortex but a sequence of vortices it does make sense to look at the effect of these vortices from a time-averaged point of view. To do so, all footprint depths for all spatial locations are time-averaged with a first order filter with a cut-off frequency corresponding to 15 vortices passing the location of averaging. As a result a typical development in form of an envelope of the size of the footprints is obtained.

Fig. 5 displays these streamwise time-mean envelopes for a long-time average. Pressure fluctuation envelopes p_{env} are made dimensionless by the free-stream dynamic pressure $q = 1/2\rho U_\infty^2$. If all envelopes are centered around $\overline{x}_R$ no differences are seen between the actuated and the unactuated cases. All phases of the vortex evolution, i.e. unstable growth, limitation before the reattachment position and finally decay, are

reflected in this graph.

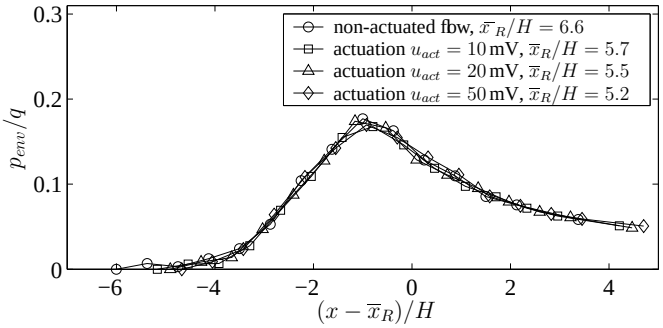

Figure 5: Streamwise time-mean envelopes p_{env} of the vortex footprints (experiment with $Re_H = 4000$)

As forced und unforced envelopes coincide this suggests the following sensor concept. From Fig. 5 it can be seen that all envelopes have identical p_{env}-values some distance down the reattachment location $x = \overline{x}_R$. Take as an example a constant $p_{env,0}$-value four step heights down the reattachment point. Starting from this value p_{env} develops exponentially according to

$$\dot{p}_{env} = K p_{env} \tag{2}$$

with K taken from Fig. 5. As the position in the unnormalized coordinate x where $p_{env} = p_{env,0}$ varies and is a function of the actuation this position and hence the reattachment location four step heights downstream can be estimated by a Kalman filter.

Fig. 6 illustrates the principle of the pattern recognition filter. First the filter is initialised four step heights H upstream of the reattachment position estimated in the prior step, see the square at $p_{env,0}$. The temporal averaged pressure envelopes p_{env} at the microphone positions, see the circles, are utilized for the measurement updates of the Kalman Filter simulation plotted as a thick solid line. If the probability density of an innovation of the Kalman filter falls under a certain limit the end of the exponential growth phase is reached, see the downstream end of the thick solid line. A clear separation of the exponential growing phase from the downstream limitation phase is possible exploiting this probability density. Going back to the last used updated position and performing a backward simulation to the constant initial value $p_{env,0}$ with Eq. 2 a new initial position is obtained, see the dashed line in Fig. 6. This new position plus four step heights H gives the new estimate of the reattachment length x_R. It is used for the initialisation of the next Kalman filter. This reattachment length x_R is used for control.

Both the reattachment and the initial position are corrected in every filter step. Thus the algorithm is able to follow flapping motions as well as actuation induced motions of the reattachment position. In Fig. 6 a scene during the reduction of the reattachment length x_R by an actuation step is shown as a correction $\Delta x/H$ is proposed towards lower values.

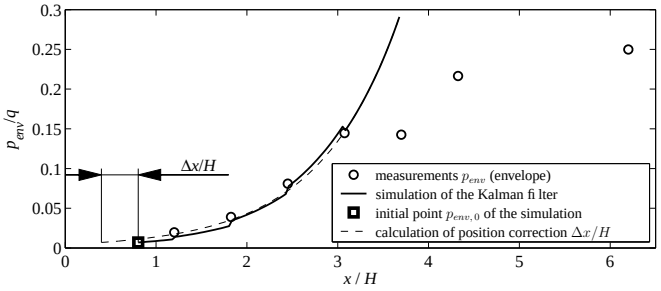

Figure 6: Streamwise observation of the exponential growth phase utilizing the temporal averaged envelope p_{env} of the vortex convection mode (simulation with $Re_H = 4000$). The estimated correction $\Delta x/H$ of the initial position also gives the correction of the reattachment position x_R.

To find out the new sensor's accuracy and dynamics the estimated reattachment positions are compared to the known positions from simulated data. However, as the instantaneous simulated data show very irregular patterns with forward- and backward-flowing spots and irregularities in the spanwise z-direction the reattachment length in a zone is considered. This zone extends $\pm 1\,H$ in the spanwise direction around the centerline where the microphones are installed. From this zone the lowest and the largest values of $x_R(z)$ are extracted.

The result is shown in Fig. 7. The sensor algorithm is able to give both the dynamics of the step response and the flapping motion in the spanwise range $\pm 1\,H$. This result is also obtained with a stronger actuation step as well as with simulated step responses with a Reynolds number $Re_H = 2500$.

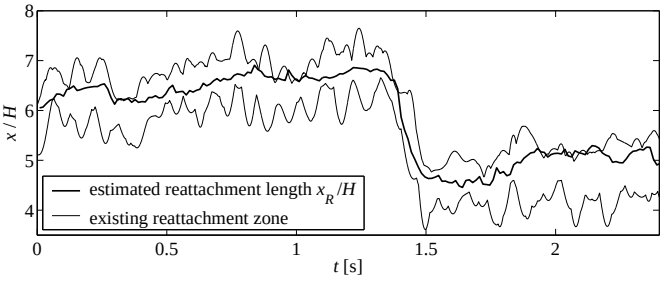

Figure 7: Comparison of estimated and existing reattachment length (simulation of step response, $Re_H = 4000$)

3.2 Controller synthesis

The determination of a controller for the tracking of the reattachment length x_R that guarantees stability and robustness is considered next. The same procedure was used in Becker et al. [2] first. A $\mathcal{H}_\infty$-controller is synthesised on the basis of a linear nominal model with a multiplicative uncertainty description. Both the nominal model and the uncertainty description are obtained from experiments using the new sensor. As the gain of all identified models shows a highly nonlinear depen-

dence on the size of the actuation signal the inverse of the nonlinear stationary gain was utilized to remove this nonlinearity.

To find a trade off between the closed-loop sensitivity function giving the performance, the restriction of the magnitude of the plant input signals, and robustness the mixed sensitivity problem is solved to shape closed-loop transfer functions. Finally, the $\mathcal{H}_\infty$-controller is implemented and experimentally tested, see next section.

3.3 Experimental Results

By using the new model-based sensor algorithm fast closed-loop tracking of the reattachment length x_R is possible, too. The corresponding tracking response to Fig. 1 is plotted in Fig. 8 using the new sensor in a closed-loop setting. Observe the much shorter time span. High-frequency disturbances are not rejected because both the system's inherent limited tracking dynamics of the reattachment length and the requirement of robustness giving the limitation of closed-loop performance.

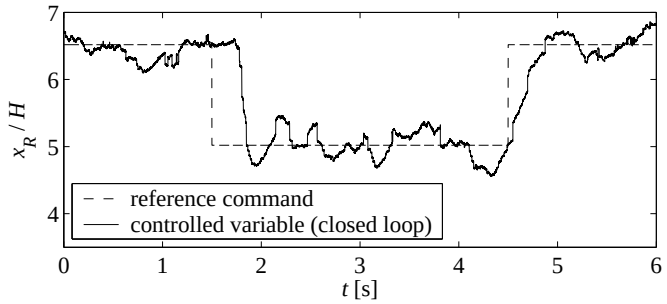

Figure 8: Tracking response of the controlled instantaneous reattachment length x_R by using the model-based sensor algorithm (experiment with $Re_H = 4000$)

4 Vortex tracking sensor

A model-based sensor algorithm which continuously estimates both the vortex positions and velocities in real-time is proposed here. The Kalman filter algorithm is used for the state estimation of the detected objects. A filter is initialised for every observed vortex. Its state is given by the object position $x(t)$ and the convection velocity $c(t)$. The detected local footprint minima at the microphone positions are used as measurement information $\underline{y}(t)$ for the filter update.

A simple stochastic state-space model for the description of the vortex convection in discrete time is given by

$$\begin{bmatrix} x \\ c \end{bmatrix}_{i+1} = \begin{bmatrix} 1 & \Delta t \\ 0 & 1 \end{bmatrix} \begin{bmatrix} x \\ c \end{bmatrix}_i + \begin{bmatrix} w_x \\ w_c \end{bmatrix}_i \qquad (3)$$

where Δt denotes the sampling interval and w_x and w_c are Gaussian white noises.

In Fig. 9 the principle of the tracking sensor is demonstrated. Simulation data are used in this figure to compare the estimated results with information which is not accessible in experiments. However, the real-time algorithm applied in experiments is used here, too. The estimated vortex courses in the pressure field p' as well as the vorticity distribution ω_z with several vortices are to be seen.

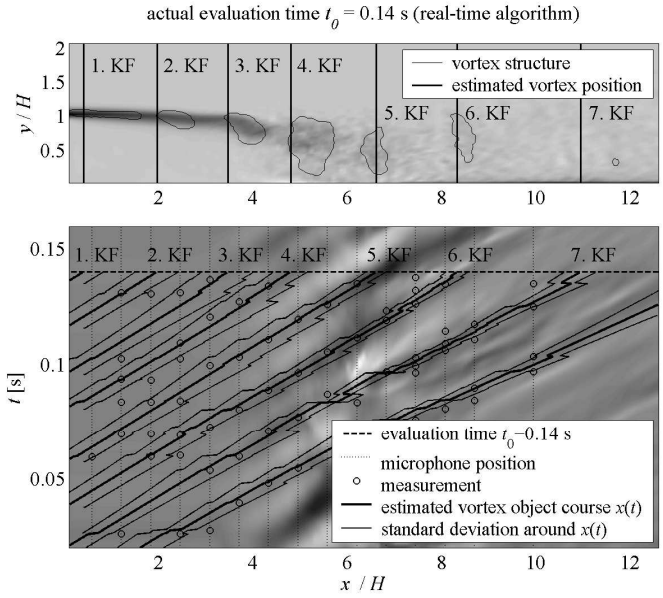

Figure 9: Estimation of multiple vortex object courses (bottom: space-time contour plot of wall-pressure fluctuations p') with Kalman filters (KF) and comparison of estimated positions of vortices with the calculated vorticity field ω_z (top)

After the Kalman filters are initialised at $x = 0$ the courses are calculated by a time update. A measurement update is performed if footprints, see circles in Fig. 9, are detected by the microphones. The estimated standard deviation around each object course $x(t)$ is displayed to give an intuitive view of the confidence of the estimations. Fig. 9 displays the status for $t = 0.14\,\mathrm{s}$ (dashed line). Earlier time points have already been evaluated and later ones are not accessible to the real-time algorithm. The updated courses in the reattachment zone $4 \lesssim x/H \lesssim 8$ match the vortex positions well (see top of figure).

To obtain a multiple target tracking algorithm two features are implemented. First, the Kalman filters are initialised in a way that the distances between the vortices correspond to the wavelength of the step mode. This procedure is triggered by a well updated vortex position. In doing so, the first filter (1. KF) in Fig. 9 was started when the position of the fifth one was found to be four times of a mean vortex distance. Second, the relation of a measured footprint to an associated filter is executed by evaluating the probability density of the innovation. Thus a detected footprint is referred to the course where the highest probability density exists.

Robust behaviour to measurement noise is obtained by a special approach for the calculation of the covariance R_i of the measurement noise. To take into account that a deep foot-

print represents a vortex position with higher probability than a small one R_i was estimated to be inversely proportional to the depth of the footprint introduced in section 3 according to $R_i \sim 1/p_{env,\,i}$.

The tracking sensor was successfully applied to simulated and experimental data with Reynolds numbers $Re_H = 4000$ and $Re_H = 5000$. Vortex footprints in both natural unforced flows and actuated cases are tracked robustly.

Motivating vortex tracking, the phase information of the periodic vortices can be exploited for a synchronisation control. Possible applications can be found in turbo-machines to reduce noise and improve efficiency by synchronising the vortex interaction with components, such as stators or rotor blades.

Additionally, the free-stream velocity U_∞ can be estimated from the vortex convection velocity, see Eq. 1, and used for the scheduling of controller parameters.

5 Conclusions and outlook

A real-time sensor algorithm for the determination of the state of the exponential vortex growing is developed on the basis of online microphone measurements. The position of this growing phase is related to the reattachment position using simulated data. Both the natural flapping motion and the actuated motion of the spatially averaged reattachment position are resolved by the model-based sensor with regard to the controllable dynamics. Subsequently, the proposed sensor is carried over to an experiment in a wind tunnel where closed-loop control is successfully implemented in real-time.

A multiple vortex tracking sensor estimates the positions and convection velocities of the coherent vortical structures. Its use for control is outlined. However, an implementation of the controller has still to be done.

Acknowledgments

This work was supported by the German Science Foundation (DFG) (collaborative research centre 557 *Manipulation of Complex Turbulent Shear Flows*).

References

[1] B.G. Allan, J.-N. Juang, D.L. Raney, A. Seifert, L.G. Pack, and D.E. Brown. Closed-loop separation control using oscillatory flow excitation. *ICASE Report No. 2000-32*, 2000.

[2] R. Becker, M. Garwon, C. Gutknecht, G. Bärwolff, and R. King. Robust control of a backward-facing step (in german). *at-Automatisierungstechnik*, 50(2):79–86, 2002.

[3] H.H. Fernholz, G. Janke, M. Schober, P.M. Wagner, and D. Warnack. New developments and applications of skin-friction measuring techniques. *Meas. Sci. Technol.*, 7:1396–1409, 1996.

[4] H. Fiedler and H.H. Fernholz. On the management and control of turbulent shear flows. *Progr. Aeronaut. Sci.*, 27:305–387, 1990.

[5] M. Gad-el-Hak, A. Pollard, and J.-P. Bonnet, editors. *Flow Control: Fundamentals and Practices*. Springer-Verlag, Berlin, 1998.

[6] M. Garwon, F. Urzynicok, L.H. Darmadi, R. King, and G. Bärwolff. Adaptive control of separated flows. *accepted for The European Control Conference ECC 2003*, University of Cambridge, UK, September 1-4, 2003.

[7] J. Gerhard, M. Pastoor, R. King, B.R. Noack, A. Dillmann, M. Morzyński, and G. Tadmor. Model-based control of vortex shedding using low-dimensional galerkin models. *accepted for the 33rd AIAA Fluid Dynamics Conference and Exhibit*, Orlando, Florida, June 23-26, 2003.

[8] M.A.Z. Hasan. The flow over a backward-facing step under controlled perturbation: laminar separation. *J. Fluid Mech.*, 238:73–96, 1992.

[9] M. Hinze. *Optimal and instantaneous control of the instationary Navier-Stokes equations*. Habilitation thesis, Technische Universität Berlin, Berlin, 2000.

[10] A. Huppertz. *Aktive Beeinflussung der Strömung stromab einer rückwärtsgewandten Stufe (in german, transl.: Active control of the flow around a backward-facing step)*. PhD thesis, Technische Universität Berlin, Berlin, 2001.

[11] M. Kiya and K. Sasaki. Structure of large-scale vortices and unsteady reverse flow in the reattaching zone of a turbulent separation bubble. *J. Fluid Mech.*, 154:463–491, 1985.

[12] I. Lee and H.J. Sung. Multiple-arrayed pressure measurement for investigation of the unsteady flow structure of a reattaching shear layer. *J. Fluid Mech.*, 463:377–402, 2002.

[13] D.G. Mabey. Analysis and correlation of data on pressure fluctuations in separated flow. *J. Aircraft*, 9:642–645, 1972.

[14] M. Pastoor, R. King, B.R. Noack, and A. Dillmann. Model-based coherent-structure control of turbulent shear flows using low-dimensional vortex models. *accepted for the 33rd AIAA Fluid Dynamics Conference and Exhibit*, Orlando, Florida, June 23-26, 2003.

[15] R. Sonnenberger. Private communication, 2002.